

# Effect of Non-Uniform Distribution of Longitudinal Reinforcement on the Behavior of Reinforced Concrete Horizontally Curved Beams with Fixed-Ends

Hayder Mohammed Kadhim Al-Mutairee  
University of Babylon /College of Engineering

## Abstract

The aim of this article is to study the effects of non-uniform distribution of longitudinal reinforcements on the behavior of reinforced concrete (RC) horizontally curved beams with fixed-ends under static loads to produce an optimal strength of these beams without increasing the volume of longitudinal reinforcement. Three dimensional nonlinear finite element analyses done utilizing computer program called *NFHCBLS*, incorporate 20-node isoparametric brick element used to represent the concrete elements while reinforcing bars are idealized as axial members embedded within the concrete elements without any relative displacement between them. The results show that the effect of non-uniform distributions of longitudinal reinforcement of RC horizontally curved beams with fixed-ends is effective and can be used to improve the strength of this type of beams and its importance increases with increasing the **angle of horizontal curvature ( $\theta$ )** of beam. The results proved that the optimal value of tapering ratio depends on  $\theta$ , for  $\theta = 30^\circ$  and  $43^\circ$ , the optimal tapering ratio obtained was equal to 7 which gives increment in the ultimate load of beam is equal to 14.5%, while when  $\theta = 56^\circ$  the optimal value of tapering ratio is equal to 3 which gives increment in the ultimate load is equal to 27.5%. So, all optimal values of tapering ratio are compatible with the value of **angle of strengthening the positive reinforcement ( $\phi$ ) = 0.75 $\theta$**

## الخلاصة

الهدف من هذا البحث هو دراسة تأثيرات التوزيع غير المنتظم للتسليح الطولي على تصرف الأعتاب الخرسانية المسلحة المنحنية أفقياً و ذات النهايات الثابتة تحت تأثير أحمال استاتيكية لأستحصال المقاومة المثلى لهذه الأعتاب دون زيادة حجم التسليح الطولي. تحليلات العنصر المحدد اللاخطية ثلاثية الأبعاد تمت بالإستفادة من البرنامج الحاسوبي المسمى *NFHCBLS* المتضمن استخدام العنصر الطابوقي ذي العشرين عقدة لتمثيل العناصر الخرسانية أما حديد التسليح فقد مثل بعناصر محورية مطمورة داخل العناصر الطابوقية للخرسانة مع افتراض عدم وجود أراحة نسبية بينهما (أي وجود ترابط تام بين الخرسانة وحديد التسليح). النتائج بيّنت أن تأثير التوزيع غير المنتظم للتسليح الطولي للأعتاب الخرسانية المسلحة المنحنية أفقياً و ذات النهايات المثبتة فعال ويمكن استخدامه لتحسين مقاومة هذه النوع من الأعتاب وأهميته تتزايد مع تزايد زاوية الانحناء الأفقي ( $\theta$ ) للعتب. النتائج أثبتت إن القيمة المثلى للنسبة المُستدقة تعتمد على  $\theta$ ، عند  $\theta = 30^\circ$  و  $43^\circ$  فإن نسبة الأستدقاق المثلى المستحصلة كانت مساوية 7 حيث تعطي زيادة في الحمل الأقصى للعتب مساوية إلى 14.5% بينما عندما تكون  $\theta = 56^\circ$  فإن القيمة المثلى لنسبة الأستدقاق تساوي 3 حيث تعطي زيادة في الحمل الأقصى للعتب مساوية إلى 27.5%. كذلك إن كل القيم المثلى لنسب الأستدقاق متوافقة مع زاوية تقوية التسليح الموجب المساوية ( $\phi$ ) المساوية إلى 0.75 $\theta$ .

## 1- Introduction

### 1.1 Previous Researches

Reinforced concrete (RC) horizontally curved beams are frequently used in bridges, because the constraints of existing land use and also used in buildings due to the architectural and structural requirement. [Jordaan et al., 1974] presented a plastic analysis methods for determination the collapse loads of RC circularly curved beams, the longitudinal reinforcement used in the experimental tests were uniform along the length. [Badawy et al., 1977] presented experimental and analytical studies to investigate the applicability of plastic methods to predict the ultimate load and failure mode of a RC horizontally curved beam, as well as the effect non-uniform distribution of shear reinforcement along the curved beam. [Bathe and Ramaswamy, 1979] presented the formulation and numerical implementation of a three-dimensional (3D) concrete model. The model adopted employs three basic features to describe the material behavior: 1-a nonlinear stress-strain relation including strain-softening to allow for the weakening of the material, 2-a failure envelope that defines cracking in

tension and crushing in compression, and 3-a strategy to model the post-cracking and crushing behavior of material. [Cervera et al., 1987] describes an efficient and accurate 3D finite element model which may be adopted in the nonlinear analysis of RC structures incorporate 20-node and 8-node isoparametric solid elements. [Al-Shaarbaf, 1990] presented a 3D nonlinear finite element model suitable to analyze the RC structures under static loads. The compressive behavior of the concrete was simulated by an elasto-plastic work hardening model followed by a perfectly plastic plateau which is terminated at the onset of the crushing. The analysis stopped at the first crushing of any Gauss point. [Al-Sherrawi, 2001] studied the nonlinear response of composite beams by using the finite element method. A two dimensional plane stress finite element method is used to simulate the concrete. The material nonlinearities as a result of nonlinear response of concrete in compression, crushing and cracking of concrete, yielding of reinforcement bar, shear-slip and dowel action between the precast concrete beams and cast-in-situ slabs were presented. Recently, [Al-Mutairee, 2008] investigates the analysis of 3D horizontal beam (steel, concrete and composite) subjected to static and dynamic loads. For concrete beams, the effect of tapering ratios and curvature were taken into account on the behavior and dynamic response of curved beams. Among many conclusions of static analysis, the investigation showed that when the effect of crushing was ignored the difference between the analytically predicted ultimate loads and the experimental data increased from 0% to 40%. [Raad, 2009] studied the effect of the width to depth ratio ( $bf/d$ ) and the curvature of the steel I-section horizontally curve beams on their ultimate strength. The research adopts 3D nonlinear finite element analysis of steel I-section horizontally curved beams under static load. The 20-node isoparametric brick element has been used to represent the steel element. The results appear that the ( $bf/d$ ) ratio equal to 1.5-2 is optimum for different values of curvature.

### **1.2 Objective of the Research**

As shown all previous investigations and studies did not appear the effects of non-uniform distribution of longitudinal reinforcement on the behavior of RC horizontally curved beam. Therefore, the main object of this research is to study this effect. This effect is very important to achieve best strength and performance of RC horizontally curved beam without increasing the volume of reinforcement.

### **2- Nonlinear Finite Element Program**

The computer program coded **NFHCBSL** (Nonlinear Finite element analysis of **H**orizontally **C**urved **B**eam under **S**tatic **L**oad) presented by [Al-Mutairee, 2008] adopted in this paper. The finite element idealization, models of materials, Numerical Integration and nonlinear solution technique used in this program illustrated in appendix A.

### **3- Reliability of Program**

To evaluate the reliability of the program a RC fixed ended horizontally curved beam tested experimentally by [Jordaan et al., 1974], coded (C3) will be analyzed. Owing to the geometric and loading symmetry, the analysis was carried out for half of the beam. All properties of materials and the parameters adopted in the analysis are as detailed in Table (1). Fig.(1) shows the loading conditions. The nodes located at the perimeter of the ends will be considered fixed, while the nodes located at mid-span will be restrained in the tangential direction only. A convergence study of this curved beam (C3) was done by [Al-Mutairee, 2008] including seven different meshes involving a total of 68, 84, 100, 116, 132, 148 and 160 elements. The results show that the difference between any successive meshes decreased until it is reached to 1%

between 148 element and 160 element meshes. Thus the mesh of 148 is adopted in the previous and current analyses.

**Table (1): Properties of Materials and Parameters Adopted in the Analysis.**

Materials Properties		Parameters
The compressive strength of concrete (cylinder) MPa	$f'_c = 41.4$	$\alpha_1 = 40$
The yield strength for longitudinal reinforcements MPa	$f_{yl} = 384.0$	$\alpha_2 = 0.4$
The yield strength for stirrups reinforcements MPa	$f_{ys} = 240.0$	$\gamma_1 = 10$
The modulus of elasticity MPa	$E_c = 30,241$	$\gamma_2 = 0.5$
The tensile strength of concrete MPa	$f_t = 1.885$	$\gamma_3 = 0.1$
Concrete: $\nu = 0.2, \varepsilon_u = 0.0035$ . Reinforcement: $\nu = 0.0, \varepsilon_u = 0.20$		Cp=0.3
The modulus of elasticity of steel GPa	$E_s = 200$	Tole.= 0.15%

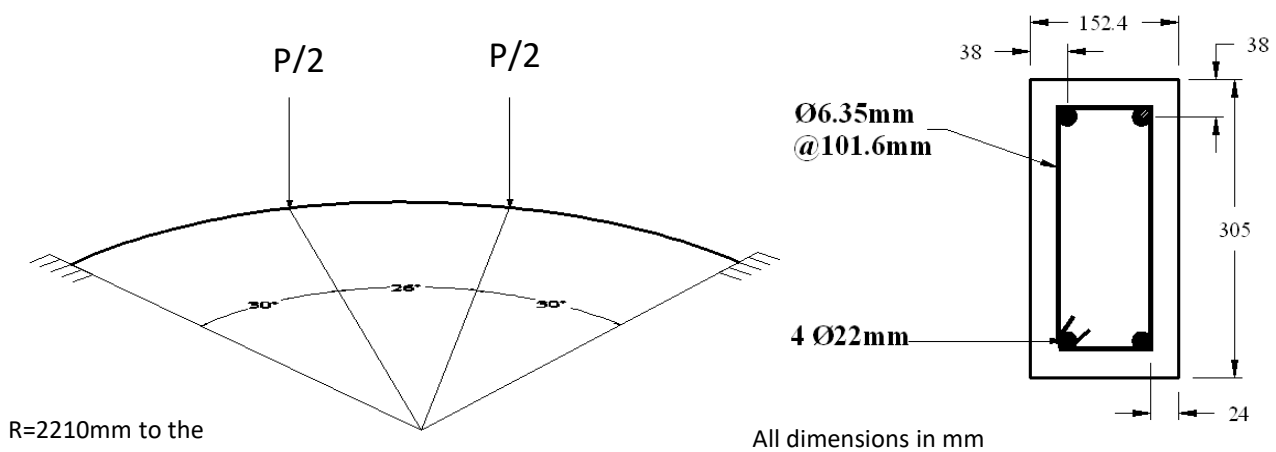


**Figure (1): Geometry and Loading Conditions of Jordaan *et al.* Curved Beam (C3).**

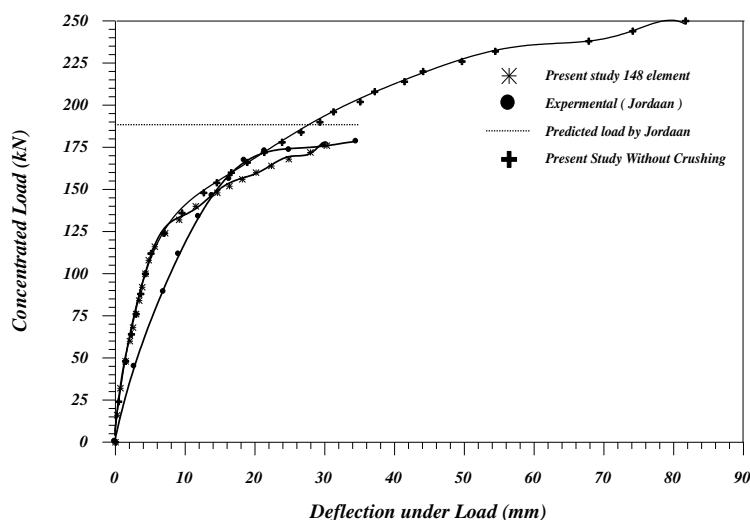


**Figure (2): Load – Deflection Curves for Jordaan et al. RC Horizontally Curved Beam (C3).**

In general, good agreement is obtained between experimental and analytical load-deflection curves as shown in Fig.(2). The obtained results appeared that the predicted ultimate load coincided with the experimental that equal to (178 kN), while the predicted ultimate load by Jordaan et al. was 188 kN. The analysis showed that the importance of considering the crushing phenomena, where if the crushing ignored the obtained ultimate load was equal to 250 kN, i.e. the difference between predicted load and experimental value is equal to 40%. Also the results showed that rupture occurred in reinforcement bars near to the fixed end, see Fig.(3), consequently the collapse mechanism happened.

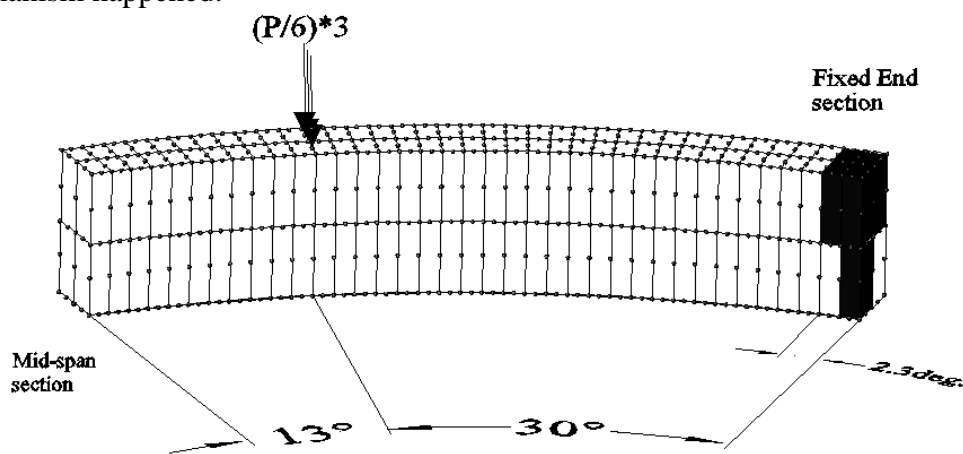


**Figure (3): The Elements Suffer from the Ruptured of Longitudinal Reinforcement.**

#### **4- Effect of Non-Uniform Distribution of Longitudinal Reinforcement on the Behavior of Reinforced Concrete Horizontally Curved Beams**

##### **4.1 Parametric Study**

A parametric study incorporate redistribution the longitudinal reinforcement along the curved beam by increasing the area of steel at the critical sections and decreasing it at other sections had been done. As shown in Fig.(3) the area of

reinforcement will be increased at the maximum tensile strength regions, the top reinforcement at the fixed end and the bottom reinforcement at the mid-span, while the other reinforcement will be decreased. In order to study this effect, thirty beams with constant length, cross-sectional area of concrete, sum of total area of longitudinal reinforcement, area of stirrups, properties, parameters, case of loads and boundary condition are studied (the same values of previous example Jordaan et al. (C3)). The values of *angle of curvature* ( $\theta$ ) were  $30^\circ$ ,  $43^\circ$  and  $56^\circ$ , for each value of  $\theta$ , three values of tapering ratios will be studied, these are 1.667, 3 and 7 (according to the increments and decrements in the area of reinforcement which equals to  $\pm 25\%$ ,  $\pm 50\%$  and  $\pm 75\%$  respectively, however, the sum of area of longitudinal reinforcement still constant at any section and equal to  $760 \text{ mm}^2$ , note: tapering ratio means here that the larger area of reinforcement over the smaller area). For each tapering ratio three values of *angle of strengthening the positive reinforcement* ( $\varphi$ ) ( $25\% \theta$ ,  $50\% \theta$  and  $75\% \theta$ ) investigated, see Fig. (4), as well as the prismatic cases (case for each  $\theta$ , tapering ratio equal to one and  $\varphi = 0$ ). Thus, each angle of curvature contains ten cases of study. Figures (5), (6) and (7) represent the results of all these thirty cases for  $\theta = 30^\circ$ ,  $\theta = 43^\circ$  and  $\theta = 56^\circ$  respectively. Each case required 10012 input data, where the analytical half beam consists of 1131 nodes, 184 elements and 284 segments of reinforcement. For all cases of studies  $\omega = 0.3 \theta$

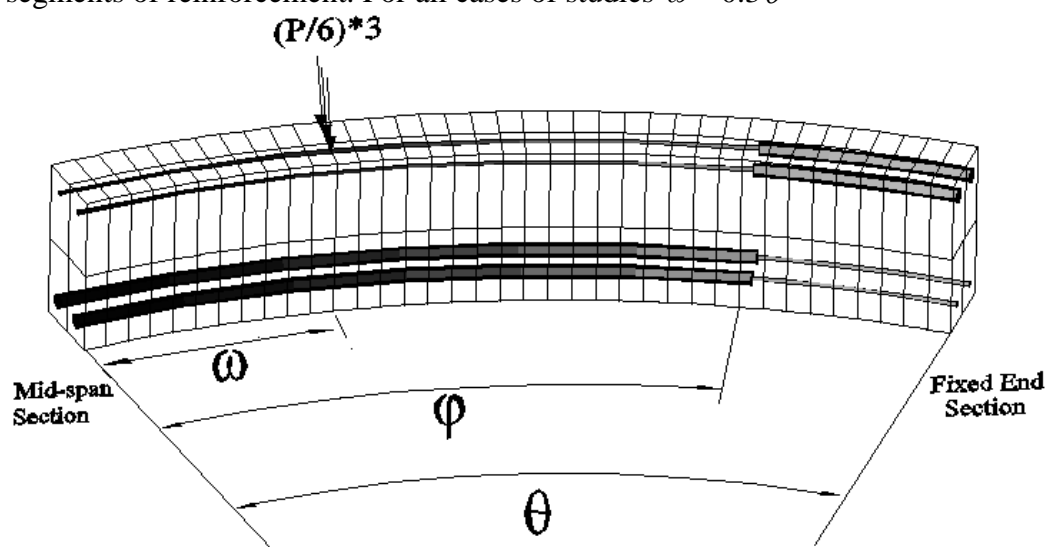


Figure (4): Locations of Increments and Decrements of Longitudinal Reinforcement.

## 4.2 Discussion of Results

### 4.2.1 Tapering Ratio is Equal to 1.667 ( $475 \text{ mm}^2 / 285 \text{ mm}^2$ )

As shown in Figs.(5-a), (6-a) and (7-a), the strength of the RC curved beam decreases for any value of  $\varphi$  if  $\theta = 30^\circ$ , but it increases with increasing of  $\varphi$  when  $\theta = 43^\circ$  or  $\theta = 56^\circ$ , also, the figures appear the performance improvement of curved beams against the deflection for all values of  $\varphi$  and  $\theta$ . Maximum increment in the ultimate strength due to non-uniform distribution of longitudinal reinforcement was 9% at  $\theta = 56^\circ$  and  $\varphi = 42^\circ$ .

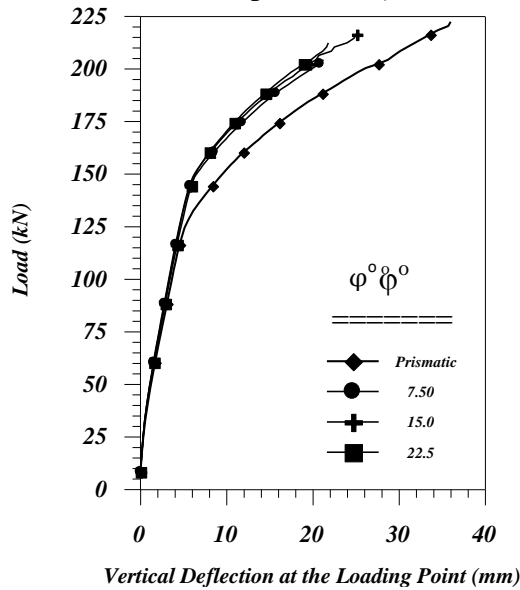
### 4.2.2 Tapering Ratio is Equal to 3.000 ( $570 \text{ mm}^2 / 190 \text{ mm}^2$ )

The results of this tapering ratio proved that improvement in the strength of RC curved beams against deflection and loads except the case of ( $\theta = 30^\circ$  with  $\varphi = 7.5^\circ$ ) as shown in Figs.(5-b), (6-b) and (7-b). It is nice to note that the gain of the non-

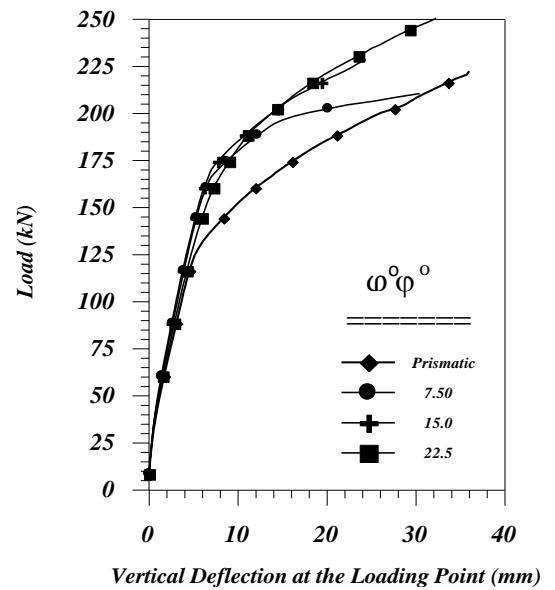
uniform distribution of longitudinal reinforcement increases with  $\theta$ , for example, the increment in the ultimate load is equal to 13.6%, 14.5 % , 27.5 for  $\theta = 30^\circ, 43^\circ, 56^\circ$  respectively (for  $\varphi = 0.75\theta$ , i.e.  $\varphi = 22.5^\circ, 32.5^\circ, 42^\circ$  respectively). Also it is important to note that the deflections of RC curved beams with  $\varphi = 0.75\theta$  were larger than the deflections when  $\varphi = 0.50\theta$  or  $0.25\theta$  because the decreasing in the region of  $(\theta - \varphi)$  produce a weak negative moment region which leads to increase the deflection

4.2.3 Tapering Ratio is Equal to 7.000 ( $665\text{mm}^2/95\text{mm}^2$ )

Here the secondary reinforcement will be thin therefore when ( $\varphi = 0.75\theta$ ), see Figs. (5-b), (6-b) and (7-b), the deflections of non- uniform distribution were larger than the deflection of prismatic (uniform distribution ) and the differences among them increase with  $\theta$ . Optimal of  $\varphi = 0.50\theta$  for any value of  $\theta$ .



(a)-Tapering Ratio=1.667



(b)-Tapering Ratio=3.000

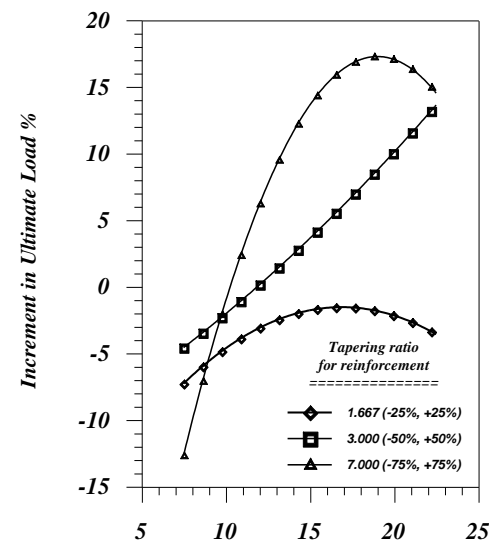
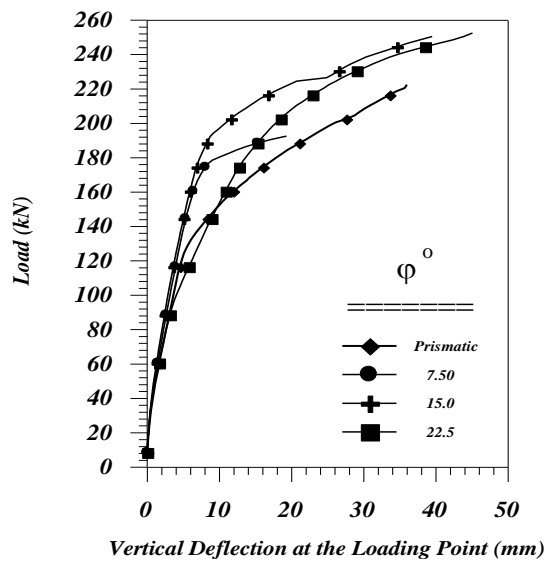
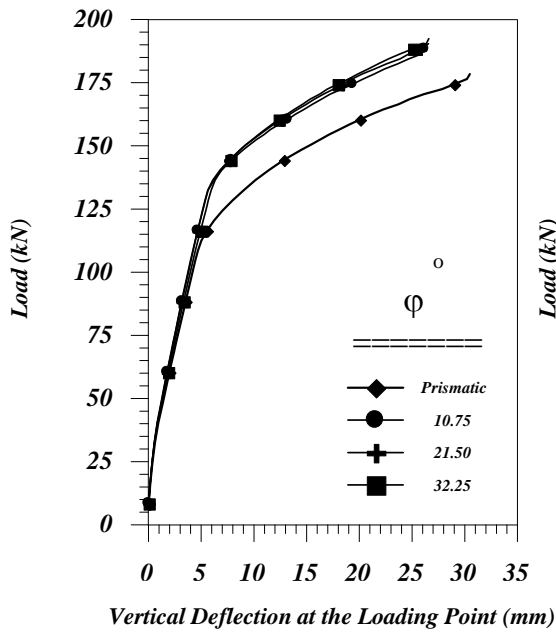
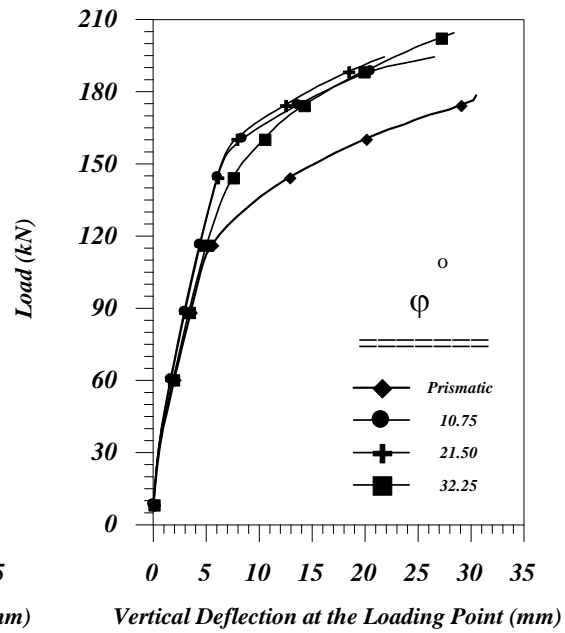


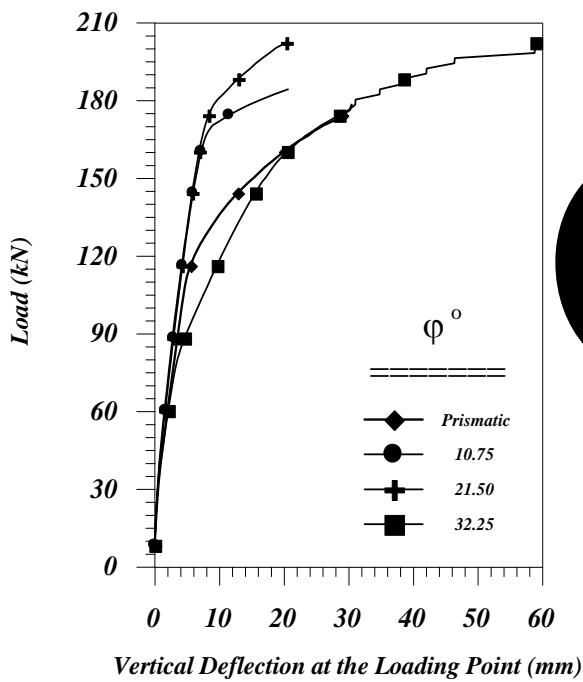
Figure (5): (a,b,c)-Load Deflection Curves of Reinforced Concrete Curved Beam: (d)- Increment Angle Curves of Reinforced Concrete Curved Beam,  $\theta=30^\circ$ .



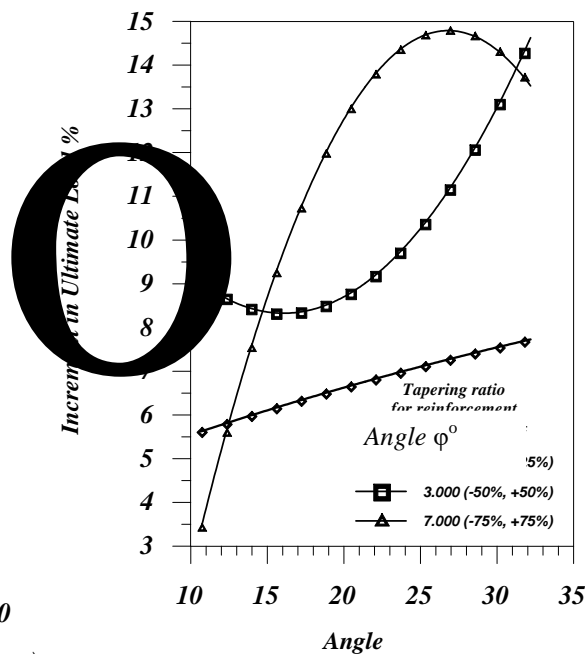
(a)-Tapering Ratio=1.667



(b)-Tapering Ratio=3.000

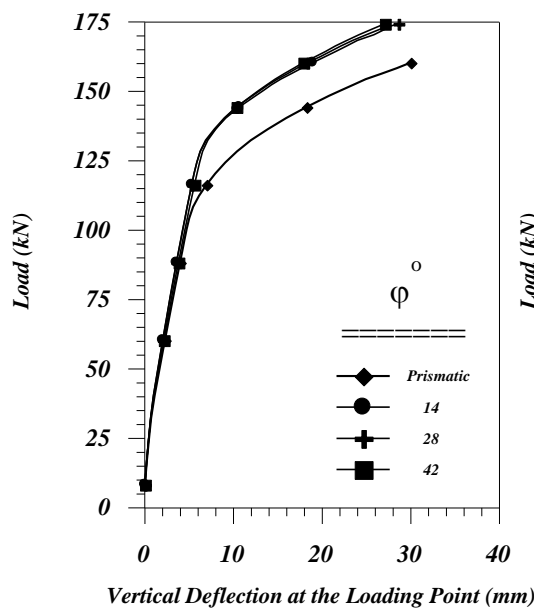


(c)-Tapering Ratio=7.000

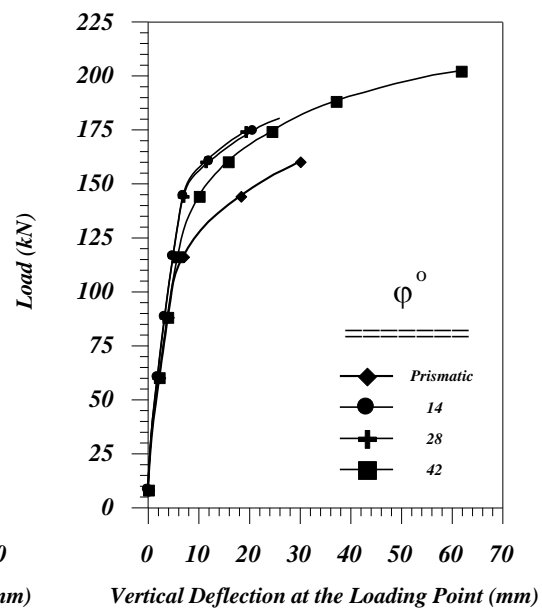


(d)-increment- $\phi$  Curves

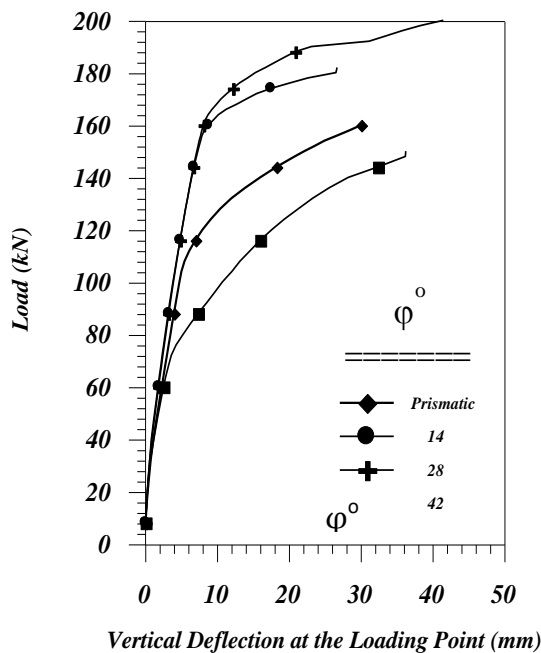
Figure (6): (a,b,c)-Load Deflection Curves of Reinforced Concrete Curved Beam: (d)-Increment Angle Curves of Reinforced Concrete Curved Beam,  $\theta=43^\circ$ .



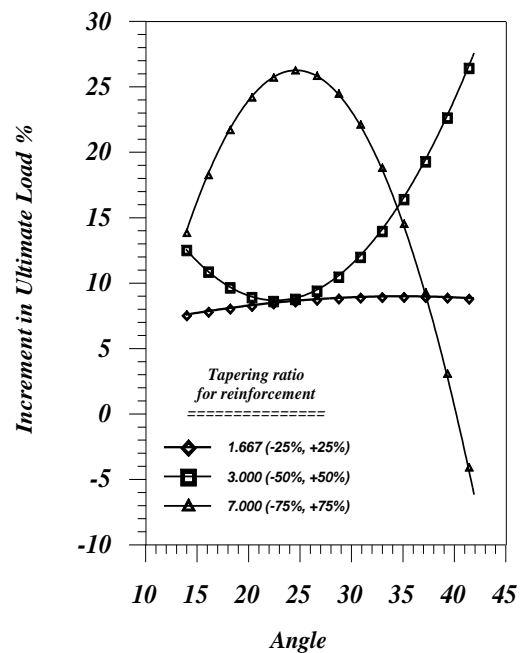
(a)-Tapering Ratio=1.667



(b)-Tapering Ratio=3.000



(c)-Tapering Ratio=7.000



(d)-increment- $\phi$  Curves

Figure (7): (a,b,c)-Load Deflection Curves of Reinforced Concrete Curved Beam: (d)-Increment Angle Curves of Reinforced Concrete Curved Beam,  $\theta = 56^\circ$ .

## 5- Conclusion

Based on the analytical results obtained from thirty case of study, the following conclusion can be drawn for fixed-ends RC horizontally curved beams:

- 1- The effect of non-uniform distributions of longitudinal reinforcement of RC horizontally curved beam with fixed-ends is effective and can be used to improve the strength of beams, and its importance increases with increasing the *angle of horizontal curvature* ( $\theta$ ) of the beam. Also, it always improves the resistance of beams against deflection except the case when ( $\theta = 56^\circ$ ) with (*angle of strengthening the positive reinforcement*,  $\varphi = 0.75\theta$  i.e.  $42^\circ$ ).
- 2- The optimal value of tapering ratio depends on  $\theta$ , for  $\theta = 30^\circ$  and  $43^\circ$  the optimal tapering ratio is equal to 7 which gives increment in the ultimate strength equal to 14.5%, while when  $\theta = 56^\circ$  the optimal value of tapering ratio is equal to 3 which gives increment in the ultimate strength equal to 27.5%. All optimal values of tapering ratio are compatible with the value of  $\varphi = 0.75\theta$ .
- 3- If the angle of curvature (of half beam,  $\theta \leq 30^\circ$ ), the designer must take tapering ratio larger than three and ( $\varphi \geq 0.50\theta$ ) to achieve improvement in the strength and performance of beam.
- 4- If the angle of curvature (of half beam,  $\theta \geq 56^\circ$ ), the designer must take tapering ratio equal to three and ( $\varphi \leq 0.50\theta$ ) to achieve improvement in the strength and performance of this type of beams.
- 5- Finally, when  $\theta$  increases, the ultimate loads of beam decreases for any value of tapering ratio or  $\varphi$ .

## 6- References

- Al-Mutairee H.M.K., 2008, "Nonlinear Static and Dynamic Analysis of Horizontally Curved Beams", Ph.D Thesis, University of Babylon.
- Al-Shaarbaf I. A. S., 1990, "Three-Dimensional Nonlinear Finite Element Analysis of Reinforced Concrete Beams in Torsion", Ph.D Thesis, University of Bradford.
- Al-Sherrawi, M. H. M., 2001, "Shear and Moment Behavior of Composite Concrete Beams", Ph. D. Thesis, University of Baghdad, Iraq.
- Badawy H. E. I., McMullen A. E. and Jordaan, I. J., June 1977, "Experimental Investigation of the Collapse of Reinforced Concrete Curved Beams", Magazine of Concrete Research, Vol. 29, No. 99, pp. 59-69.
- Bathe K. J. and Ramaswamy S., 1979, "On Three Dimensional Nonlinear Analysis of Concrete Structures", Journal of Nuclear Engineering and Design, 52(1979), pp. 385-409.
- Cervera M., Hinton E., and Hassan O., 1987, "Nonlinear Analysis of Reinforced Concrete Plate and Shell Structures Using 20-Noded Isoparametric Brick Elements", Journal of Computers & Structures, Vol.25, No. 6, pp. 845-869.
- Cervera M., Hinton E., Bonet J. and Bicanic N., 1988, "Nonlinear Transient Dynamic Analysis of Three Dimensional Structures - A Finite Element Program For Steel and Reinforced Concrete Materials", pp. 320-550.in Hinton E. Book's, "Numerical Methods and Software for Dynamic Analysis of Plates and Shell", Prinerdge Press, 550, pages, ISBN, 0-906674-48-4.
- Cook R.D., 1974, "Concept and Application of Finite Element Analysis", John Wiley and Sons, Inc., New York.
- Hughes B. P. and Chapman G. P., March, 1966, "The Deformation of Concrete and Micro Concrete in Compression and Tension with Particular Reference to

- Aggregate Size”, Magazine of Concrete Research, London, Vol.18, No.54, pp. 19-24.
- Jordaan I.J., Khalifa M.M.A. and McMullen, A.E., Nov. 1974, “Collapse of Curved Reinforced Concrete Beams”, Journal of ASCE, Vol.100, No.ST11.
- Phillips D.V. and Zienkiewicz O.C., 1976, “Finite Element Nonlinear Analysis of Concrete Structures”, Proceedings, Institution of Civil Engineers, Vol.61, Part2, pp.59-88.
- Pognani T., Slater J., Aneur-Mosor R. and Boyukozurk O. , 1992, “ A Non-linear Three-Dimensional Analysis of Reinforced Concrete Based on Bounding Surface Model”, Computers & Structures, Vol.43, No.1, pp.1-12.
- Raad K.H., 2009, “Effect of Width/Depth (Bf/D) Section Ratio and Curvature on the Behavior of Horizontally Curved Steel Beam”, Journal of Babylon University, Vol. 17, No.3.
- William W. J. and Paul R. J., 1987, “Structural Dynamic by Finite Elements”, Prentice-Hall, INC., Englewood Cliffs, New Jersey.
- Zienkiweicz O.C., 1977, “The Finite Element Method”, Third Edition, Mc Graw. Hill, London.

### **Appendix A: Notations**

- $\theta$  = angle of horizontal curvature of horizontally curved beam, degree.
- $\varphi$  = angle of strengthening the positive reinforcement, degree.
- $C_{pt}$  = plasticity coefficient.
- $\alpha_1$  = rate of post-cracking stress decay as the strain increases.
- $\alpha_2$  = sudden loss in stress at instant of cracking.
- $\epsilon_u$  = ultimate compressive strain of concrete at which crushing occurred.
- $\rho_{pw}$  = ratio of positive reinforcement for short direction.
- $\epsilon_{cu}$  = crushing strain of concrete = 0.003.
- $\nu$  = Poisson’s ratio.
- $\omega$  = angle of applying the concentrated load on curved beam.
- $\gamma_1$  = rate of decay of shear modulus as the crack widens.
- $\gamma_2$  = sudden loss in the shear modulus at the onset of cracking.
- $\gamma_3$  = residual shear modulus due to the dowel action.

### **Appendix B: Finite Element Idealization and Modeling of Materials**

#### **B-1: Concrete Idealization**

In the present study, the 20-node quadratic brick element has been adopted for describing the concrete elements. This element has been successfully used in many three dimensional nonlinear studies [Cervera et al., 1986], [Al-Shaarbaf, 1990] and [Al-Mutairee, 2008]. The element has its own local coordinate system, r, s, t as shown in Fig.(B-1), with the origin at the center of the element hence each local coordinate ranges from (-1) to (+1). For an element of volume V, the stiffness matrix can be obtained [William and Paul, 1987].

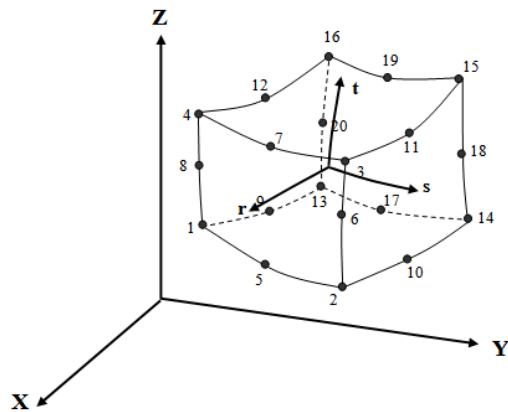


Fig.(B-1): The 20-Node Brick Element in Cartesian Coordinates.

**A-2: Reinforcement Representation**

A bar element is considered to be embedded inside the brick element parallel to r axis and has a position  $s = s_i$  and  $t = t_i$ , as shown below. The stiffness matrix of an axially loaded bar element was constructed as illustrated in reference [Phillips, and Zienkiewicz, 1976].

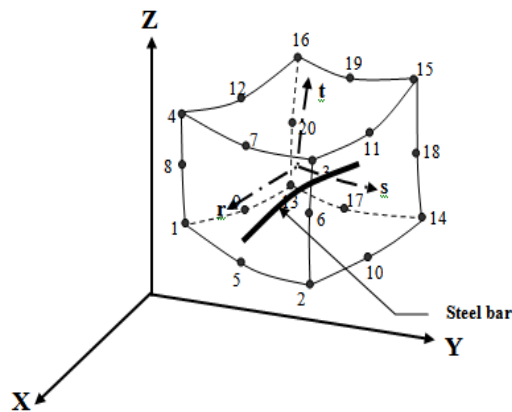


Fig.(B-2): Representation of Embedded Reinforcement.

**B-3: Concrete Model Adopted in the Static Analysis**

**B-3-1: The yield criterion used for concrete**

In the present study, a relationship between stress and strain shown in Fig.(B-3) is used. The value of 0.3 is assumed for plastic coefficient  $C_p$  for normal strength concrete. The plastic yielding begins at a stress level of  $C_p f'_c$ .

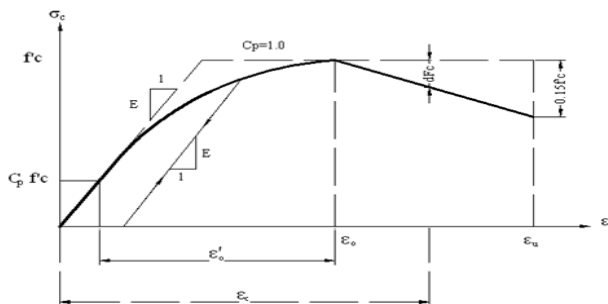


Fig.(B-3): Uniaxial Stress-Strain Curve of Concrete in Compression.

**B-3-2: The crushing condition**

In present models, it is assumed that the crushing surface in the strain space is related to a maximum equivalent strain extrapolated from uniaxial tests. Therefore the following failure surface can be used [Cervera et al., 1988]:

$$\sqrt{3J'_2} = \varepsilon_{cu} \quad \dots\dots\dots$$

(B-1) Where,  $J'_2$  is the second deviatoric strain invariant and  $\varepsilon_{cu}$  is the ultimate crushing strain of concrete. Also, when the crushing occurred, the stress state must be compressive and satisfied with the conditions [Hughes and Chapman, 1966]:

$$\sqrt{3J'_2} \leq -I_1/\sqrt{3}, \quad \text{and } I_1 \leq 0 \quad \dots\dots\dots$$

(B-2) However, when the sampling gauss point crushed its stresses drop abruptly to zero.

**B-3-3: The Smeared Crack Model for Concrete in Tension**

A smeared crack model with fixed orthogonal cracks is adopted to represent the fractured concrete in the current model. The limiting tensile stress required to define the onset of cracking can be calculated for the state of triaxial tensile stress and for combinations of tension and compression principal stresses as follows [Cervera et al., 1987] and [Al-Shaarbaf, 1990]:

a) for the tri-axial tension zone :  $(\sigma_1 \geq \sigma_2 \geq \sigma_3 > 0)$

$$\sigma_i = \sigma_{cr} = f_t \quad i = 1, 2, 3 \quad \dots\dots\dots \text{(B-3) b)}$$

for the case of the tension-tension-compression zone:  $(\sigma_1 \geq \sigma_2 > 0, \sigma_3 \leq 0)$

$$\sigma_i = \sigma_{cr} = f_t \left(1 + \frac{0.75\sigma_3}{f'_c}\right), \quad i = 1, 2 \quad \dots\dots\dots$$

(B-4) c) for the case of tension-compression-compression zone:  $(\sigma_1 > 0, \sigma_2 \leq \sigma_3 \leq 0)$

$$\sigma_1 = \sigma_{cr} = f_t \left(1 + \frac{0.75\sigma_2}{f'_c}\right) \left(1 + \frac{0.75\sigma_3}{f'_c}\right) \quad \dots\dots\dots$$

(B-5) where,  $\sigma_{cr}$  is the cracking stress.  $f_t, f'_c$  are the tensile and compressive concrete strength (positive values).  $(\sigma_1, \sigma_2, \sigma_3)$  are the principle stresses.

**B-3-4: A Post Cracking Stress-Strain Relationship/Tension stiffening model**

Tension-stiffening model Fig.(B-4) used; where;  $\sigma_n$  and  $\varepsilon_n$  are stress and strain normal to the crack plane,  $\varepsilon_{cr}$  is the cracking strain associated with the cracking stress  $\sigma_{cr}$ ,  $\alpha_1$  is the rate of post cracking stress decay as the strain increases,  $\alpha_2$  is the sudden loss in stress at instant of cracking. The unloading of a cracked sampling gauss point is assumed to follow a secant modulus (E1) path.

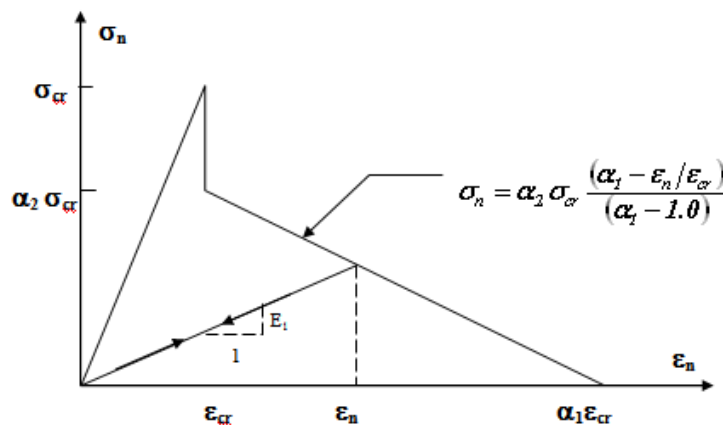


**Fig.(B-4): Post-Cracking Model for Concrete in Tension.**

### **B-3-5: Shear retention model**

The adopted shear retention model is shown below [Pognani et al., 1992], where;  $\gamma_1$  represents rate of decay of shear stiffness as the crack widens.  $\gamma_2$  represents the sudden loss in shear stiffness at onset of cracking.  $\gamma_3$  represents the residual shear stiffness due to the dowel action.

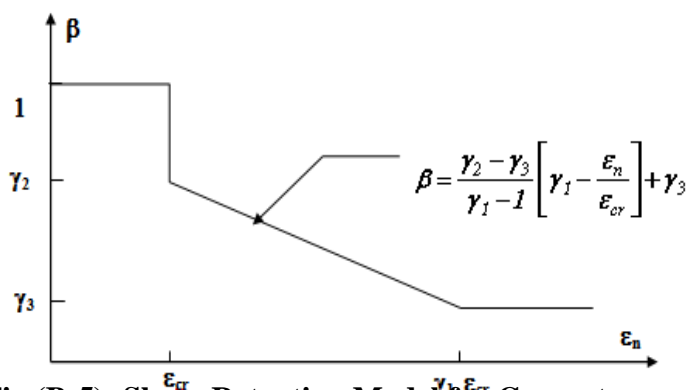


**Fig.(B-5): Shear Retention Model for Concrete.**

### **B-3-6: Modeling of Steel Adopted in the Analysis**

The elastic – perfect plastic relationship based on von-Mises criterion is used for reinforcing bars, as shown in Fig.(B-5).

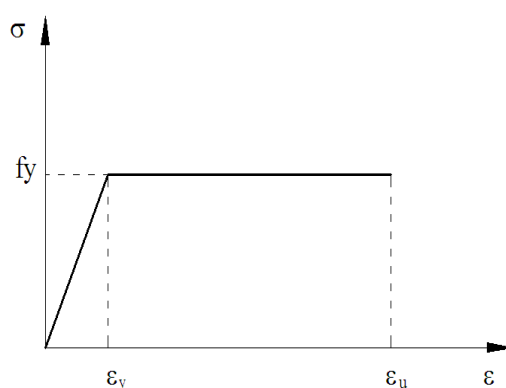


**Fig.(B-5): Idealization of Stress-Strain Curve for Steel Beams.**

### **B-4: Numerical Integration**

The Gaussian-Legendre quadratic numerical integration technique has been used to evaluate the stiffness matrix [Zienkiweixz, 1977]. The (3x3x3) Gauss quadratic integration rule has been used for concrete elements representation.

### **B-5: Nonlinear Solution Technique**

The incremental-iterative method had been used to consider the material nonlinearity problem, where the load applied as a series of increments and at each increment iterative solution is carried out to achieve the true response. At certain iteration within the increment of loading, if the difference between the external and the internal forces becomes negligibly small, the convergence is assumed to be obtained. The force convergence criterion is considered in this article.